JMEPEG (2012) 21:1320–1326
DOI: 10.1007/s11665-011-0032-z

1059-9495/$19.00

Effect of Cryogenic Treatment on AISI M2 High Speed Steel: Metallurgical and Mechanical Characterization

Simranpreet Singh Gill, Jagdev Singh, Rupinder Singh, and Harpreet Singh

(Submitted January 31, 2011; in revised form July 20, 2011)

This study aims to present the metallurgical and mechanical characterization of cryogenically treated AISI M2 high speed steel (HSS) in terms of carbide precipitation and wear behavior. The samples of commercially available conventionally quenched and tempered AISI M2 HSS were procured and subjected to cryogenic treatment at two levels −110 °C (shallow treatment) and −196 °C (deep treatment) of temperature. The microstructures obtained after cryogenic treatments have been characterized with a prominence to comprehend the influence of cryogenic treatment vis-à-vis conventional quenching and tempering on the nature, size, and distribution of carbides. The mechanical properties such as hardness and wear rate of the specimens have also been compared by performing Rockwell C hardness test and pin-on-disc wear test, respectively. Microstructures, hardness, wear rate and analysis of worn surface reveal the underlying metallurgical mechanism responsible for the improving mechanical properties of the AISI M2 HSS.

Keywords AISI M2 HSS, carbides, deep cryogenic treatment, pin-on-disc wear test, Rockwell C hardness test, shallow cryogenic treatment

1. Introduction

The life of high speed steel (HSS) cutting tools plays a major role in increasing productivity and consequently is an important economic factor. One of the major problems associated with the conventional heat treatment of these steels is the content of retained austenite (γ_{RA}), which is soft, unstable at low temperature and transforms into brittle martensite during service. Transformation of austenite to martensite causes approximately 4% volume expansion, which results in distortion of the cutting tools. The cryogenic treatment is used for minimizing the amount of γ_{RA} in tool steels. Effect of cryogenic treatment on performance of steel, particularly with respect to wear resistance, is the subject matter of quite a few research accomplishments over the last few decades. Cryogenic treatment has been claimed to improve wear resistance of several steels and has also been implemented recently in cutting tools. However, scientific research on effects of cryogenic treatment has been spotty, and only a few academic papers have been published especially on AISI M2 HSS. It has been claimed by several researchers that cryogenic treatment enhances wear resistance of some steels.

Simranpreet Singh Gill and **Jagdev Singh**, Department of Mechanical Engineering, Beant College of Engineering and Technology, Gurdaspur 143521, Punjab, India; **Rupinder Singh**, Department of Production Engineering, Guru Nanak Dev Engineering College, Ludhiana 141006, Punjab, India; and **Harpreet Singh**, Department of Mechanical Engineering, Indian Institute of Technology, Ropar 140001, Punjab, India. Contact e-mail: ritchie_223@yahoo.com.

Cryogenic treatment, the discipline on which this study is based, can be considered a recent development (Ref 1-8). Enhancement of wear resistance of tool steels by cryogenic treatment has been cited in several studies (Ref 1-22). However, the available literature on the metallurgical changes conferred by cryogenic treatment lacks scientific understanding; also the contradictory results encountered lead to misunderstanding the practical application of cryogenic treatment (Ref 14-16). Some investigators argue that the improvement of wear resistance occurs solely due to transformation of γ_{RA} to martensite (Ref 1, 3, 5). Many investigators indicate that the refinement of secondary carbides is the major cause for the improvement in wear resistance by cryogenic treatment (Ref 3, 5, 9, 11); but this opinion lacks appropriate experimental evidences (Ref 3, 5, 9). The review of the literature reveals the potential of use of cryogenic treatment in improving the performance of AISI M2 HSS material from cutting tool point of view. However, the available results in the literature pertaining to wear behavior of AISI M2 HSS tool material subjected to cryogenic treatment are not coherent and the underlying postulated mechanisms for achieving improved tool life is not well crystallized. The advantage of cryogenic treatment can only be suitably exploited if the underlying mechanism is carefully unfolded in a planned manner. This study therefore aims to examine the effects of cryogenic treatment on AISI M2 HSS with respect to the nature, size, and distribution of carbide particles in the microstructure. The consequential mechanical properties, namely hardness and wear rate were also investigated.

2. Materials and Methods

2.1 Material Used

AISI M2 HSS was chosen for studying the effect of cryogenic treatment. The chemical composition of specimens as analyzed by spark emission spectrometer (Model DV-6 Baird USA) is as follows (wt.%): C 0.88, Mn 0.22, Si 0.45, Cr 4.50,

Ni 0.20, Mo 5.45, 6.55, V 2.10, Fe balance. Commercially available quenched and tempered AISI M2 HSS tool bits of size 12 × 12 × 50 mm were procured and used as work material specimens for the study.

2.2 Cryogenic Treatment

All the AISI M2 HSS specimens were classified into three different groups as conventionally quenched and tempered (CQT) with no extra treatment, shallow cryogenically treated (SCT) and deep cryogenically treated (DCT). Each group contained two specimens. The group of specimens meant for SCT was subjected to cooling at −110 °C and held at this temperature for 18 h and gradually brought back to room temperature. Similarly, the group of specimens meant for DCT was subjected to cooling at −196 °C and held for 38 h and gradually brought back to room temperature. In this study, all the specimens were cryogenically treated under dry condition where the specimens being treated were not exposed to the liquid nitrogen to eliminate the risk and damage of thermal shock. Also, in order to avoid thermal shocks from rapid cooling and heating, the specimens were cooled down and heated up slowly, to and from the shallow cryogenic temperature (−110 °C) and deep cryogenic temperature (−196 °C), over an 4 and 7 h period, respectively, with the temperature being monitored by computerized control. This gave an average heating/cooling rate of 0.5 °C/min. After this, two tempering cycles consisting of heating to 150 °C were followed to relieve the stresses induced during cryogenic (SCT and DCT) treatment. All the specimens were cryogenically treated in cryogenic processor with tempering facility (Primero Enserve, India). Figure 1 shows the cryogenic treatment cycle used to treat the specimens.

2.3 Microstructural Analysis

The microstructure of specimens were examined using both optical (Nikon: EPIPHOT 200, Japan) and scanning electron microscope (SEM, Quanta: F-200 FEI, Holland). Specimens of size 12 × 12 × 8 mm for microstructure analysis were cut from the various heat treated AISI M2 HSS bits (CQT, SCT, and DCT) by using wire-cut electric discharge machining for microstructural characterization. The specimens were then

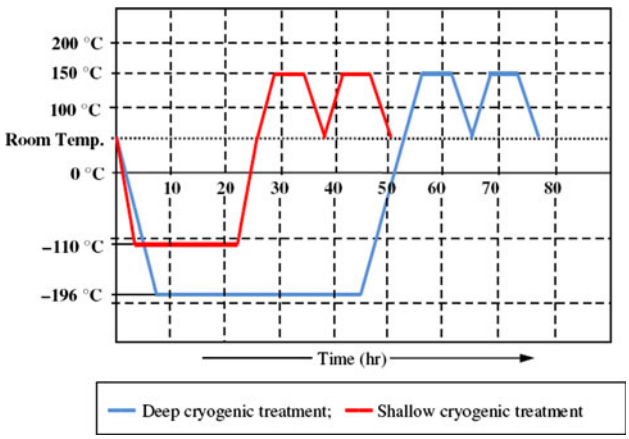

Fig. 1 Cryogenic treatment cycle used to treat the AISI M2 HSS specimens

grounded and polished by SiC abrasive papers of different grit sizes (80-1200) to make surface free from scratches. Final polishing was done on velvet cloth polishing machine with sporadic application of fine alumina dust. The surface roughness of all the samples thus produced was ensured to be about 0.01 μm. Nital with composition of concentrated nitric acid (4 mL) with ethyl alcohol (100 mL) was used for revealing microconstituents of AISI M2 HSS specimens. The quantitative determination of the carbides was done by using Leica QMetals software. The researched quantitative parameters measured in this study were total area occupied by carbides ($A_{carbide}$, %), total sum of the diameters of the carbides existing on unit area in the researched fields ($D_{carbide}$, mm), average number of the carbides on 1 mm square area ($N_{carbide}$, per mm^2) and carbides distribution on the basis of size: 0-1, 1-2, 2-4, 4-8, 8-16 μm, and >16 μm.

2.4 Hardness Test

The specimens produced for microstructural analysis as discussed in Subsection 2.3 were also used for hardness measurements. Digital Rockwell C hardness tester interfaced with computer system was used to obtain the hardness values. A minor load of 10 kg was first applied to seat the specimen. The major load of 150 kg was then applied for HRC scale for the duration of 30 s. The hardness was measured at five different points evenly distributed along the diagonal length of each specimen so as to get the average values of hardness and to evaluate any change in hardness values in the bulk of the specimen material.

2.5 Wear Test

Sliding wear tests were performed according to ASTM standard G99-05 (Ref 23) using a pin-on-disc wear testing machine (DUCOM: TR 20, India). Cylindrical pins of size φ8 × 30 mm height were cut from the heat-treated specimens of AISI M2 HSS by wire-cut electric discharge machining and the faces of the pins were grounded manually using alumina dust, and cleaned in acetone prior to wear tests. These cylindrical pins were used as static pins against En-32 steel disc (∅ 100 × 8 mm thick) as rotating counter face. These tests were carried out at loads of 49, 68.6, and 88.2 N in dry condition at sliding speed of 1.5 m/s at the room temperature. Each specimen was tested for sliding distance of about 1800 m. The wear rate of each pin was calculated from the weight loss and the each test was repeated three times for each condition to get the mean values of weight loss. The amount of wear is determined by weighing the specimen before and after the tests using a precision electronic weighing balance with an accuracy of 0.001 g. Wear rates (W_r) were calculated using the following equation:

$$W_r = \Delta m/(\rho LF) \times 10^3$$

In this equation, W_r is the wear rate (mm^3/Nm); Δm is the weight loss (g); ρ is the steel density (g/cm^3); L is the wear distance (m); and F is the normal load (N). A comparison has been made to identify the effects of each treatment (CQT, SCT, and DCT) on wear improvement. After wear tests, the worn-out surfaces of AISI M2 HSS specimen pins were cleaned by acetone. The worn surfaces of specimens were then examined under SEM (Quanta: F-200 FEI, Holland) to evaluate the governing wear mechanism.

3. Results and Discussion

3.1 Microstructure

The microstructures of the CQT, SCT, and DCT AISI m2 HSS specimens revealed the strong presence of carbide particles in tempered martensite matrix. From optical micrograph of CQT specimen shown in Fig. 2, primary carbides can easily be identified as white patches on the grayish-black martensite matrix background. However, since the optical micrograph was not able to depict the nature and size of the precipitated carbides, close range SEM images (Fig. 3) of all the specimens were obtained for evaluation of carbide phase.

It is clear from microstructures of CQT specimen (Fig. 3a) that primary carbide of somewhat dendrite structure exists in the form of clusters along with secondary carbides though the later are less in number. Some random traces of γ_{RA} can also be seen in the microstructure of CQT specimen which found out to be about 10.37%. The microstructure of SCT specimen (Fig. 3b) shows secondary carbides which might had been precipitated out during the shallow cryogenic treatment. As evident from the Fig. 3(b), the newly precipitated out secondary carbides can be classified in two categories as large secondary carbides (>4 μm) and small secondary carbides (<4 μm) on the basis of their size as proposed by Das et al. (Ref 24) for AISI D2 die steel. Still, the carbides are not evenly distributed throughout the bulk of material. It is interesting to note that the γ_{RA} was almost completely converted into martensite after subjecting the AISI M2 HSS specimen to shallow cryogenic treatment. This phenomenon may be ascribed to the fact that martensite finish temperature of AISI M2 HSS is well below room temperature because of its high carbon and alloy content; so CQT cannot transform all the austenite into martensite (Ref 25). In contrary to microstructure of SCT specimen, the microstructure of DCT specimen reveals the presence of secondary carbides which are evenly distributed in entire bulk of material. Also, the number of small secondary particles is enhanced after deep cryogenic treatment as compared to shallow cryogenic treatment. It can be inferred from the results that the size of the secondary carbides in DCT and CQT AISI M2 HSS specimens are distinctly different. This difference can be attributed to the formation of η-carbides in DCT specimens instead of ε-carbides in CQT specimens as reported by Meng et al. (Ref 15, 16). Cryogenic treatment produces internal stresses as a result of transformation of γ_{RA} to martensite and low temperature tempering of martensite. These internal stresses spawn twins and dislocations crystal lattice defects (Ref 5, 22). In addition, super saturation of martensite at cryogenic temperatures increases its lattice distortion and thermodynamic instability which promotes carbon and alloying element atoms to segregate at the nearby crystal defects. Increased population and refinement of secondary carbides with decreasing the temperature from shallow cryogenic to deep cryogenic also indicate that the precipitation behavior of carbides involves localized diffusion of carbon atoms leading to cluster formation (Ref 19). These clusters act as nuclei for the formation of small secondary carbides on subsequent tempering as observed in the microstructure of the cryogenically treated (SCT and DCT) samples. Evidently the above discussion confirms the fact that deep cryogenic treatment

Fig. 2 Optical micrograph of CQT AISI M2 HSS sample showing primary carbides as white patches and tempered martensite as grayish-black background area

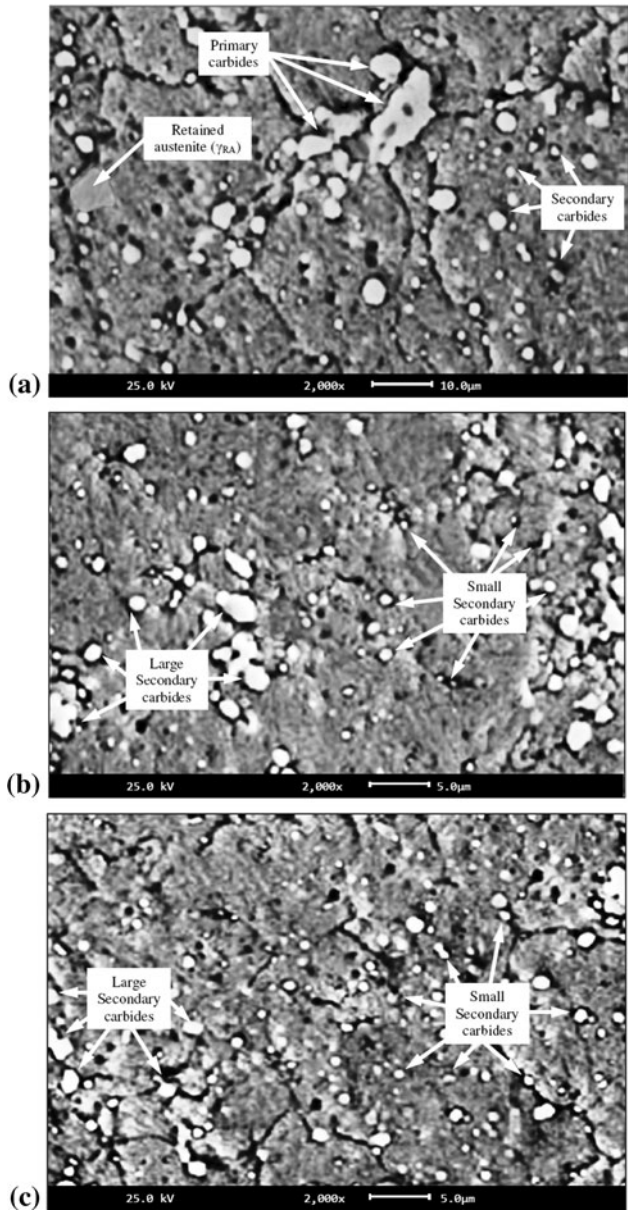

Fig. 3 Close range SEM image of (a) CQT, (b) SCT, and (c) DCT AISI M2 HSS specimens

affects the metallurgy of AISI M2 HSS by reducing the γ_{RA} amount, precipitating out and evenly distributing the small secondary carbides which may improve the mechanical properties. SEM images (Fig. 4) of the AISI M2 HSS specimen were taken for the quantitative determination of the carbides. Quantitative parameters of carbides and distribution of carbides on the basis of their size are shown in Table 1 and Fig. 5, respectively.

The critical analysis of results presented in Table 1 and Fig. 5 reveals clear differences of the carbide parameters after the application of various treatments (CQT, SCT, and DCT) on AISI M2 HSS specimens. The amount of carbides of size 0-1 μm increased by 26.76 and 34.02% as compared to conventional treatment after shallow and deep cryogenic treatment, respectively. Also, as the size of carbides goes on increasing, the percentage increase in carbide count goes on decreasing for shallow and deep cryogenic treatment up to 2-4 μm size carbides. For carbides having size larger than 4 μm, the carbide count decreased for SCT and DCT specimens as compared to CQT specimen. These outcomes are in line with the results interpreted from the SEM images and discussed earlier in this article. From the above discussions, it can be concluded that enhancement of mechanical properties such as wear resistance and hardness of AISI M2 HSS by cryogenic treatment can be attributed to the elimination of γ_{RA}, precipitation and refinement of carbide particles, and their homogeneous distribution along with secondary hardening which in a way results in favorable crack growth resistance of the material. The results of this study are consistent with previous studies that reported increase in carbide count is responsible for the improvement in wear resistance.

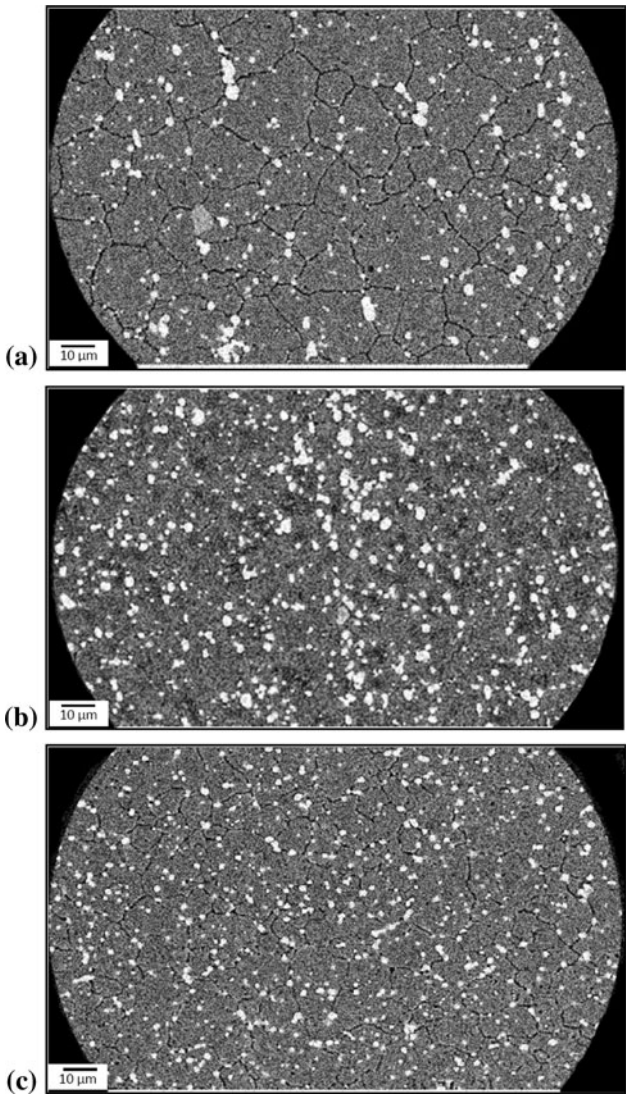

Fig. 4 SEM image used for quantitative determination of the carbides for (a) CQT, (b) SCT, and (c) DCT AISI M2 HSS specimen

3.2 Hardness

The Rockwell C (HRC) hardness values were obtained for CQT, SCT, and DCT AISI M2 HSS specimens at five equally spaced points along the diagonal length of each specimen. A plot of hardness as a function of type of heat treatment is shown in Fig. 6.

SCT AISI M2 HSS specimen has significantly higher hardness (≈7.46%) compared with that for CQT sample. Also, the improvement in hardness (≈1.47%) for DCT specimen is trivial when compared with SCT specimen. The application of shallow cryogenic treatment boosted the hardness of specimen by 5 HRC due to near complete conversion of soft γ_{RA} into relatively hard martensite. However, when the specimen was

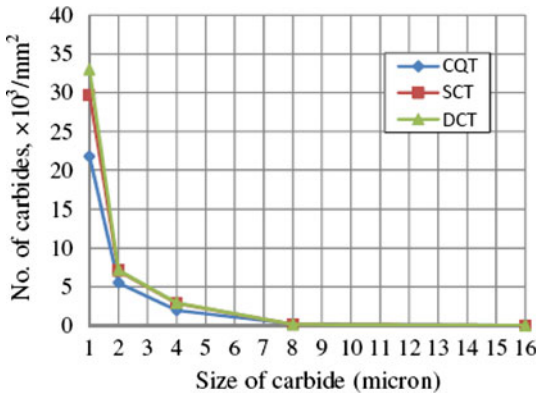

Fig. 5 Carbides distribution on the basis of carbide size

Table 1 Quantitative parameters of carbides present in AISI M2 HSS specimens

Type of heat treatment	Retained austenite (γ_{RA}), %	$A_{carbide}$, %	$D_{carbide}$, mm	Total $N_{carbide}$, mm^{-2}	Classification of carbides on the basis of size ($N_{carbide}$), mm^{-2}					
					0-1 μm	1-2 μm	2-4 μm	4-8 μm	8-16 μm	>16 μm
CQT	10.37	2.87	32.37	29,521	21,737	5533	1982	216	53	Not reported
SCT	01.64	4.93	37.74	39,871	29,683	7086	2891	164	47	Not reported
DCT	01.57	5.71	39.63	43,093	32,947	7179	2918	156	34	Not reported

subjected to deep cryogenic treatment, no major improvement was recorded in hardness as compared to SCT specimen because deep cryogenic temperature produced small secondary spherical carbides, which is important with respect to wear resistance, but may not provide significant improvement in hardness. However, any such possible increase of carbide particle density leading to higher hardness gets compensated by internal stress relaxation caused by the interactions between carbide particles and sub-structural defects. It is important to mention that near complete transformation of γ_{RA} into martensite occurred at shallow cryogenic temperature and also no further improvement in hardness was reported by further decreasing the processing temperature and increasing the processing time. Hence, it can be concluded that improvement in hardness of AISI M2 HSS specimen may primarily be attributed to the complete conversion of γ_{RA} into martensite with little contribution of precipitation of fine carbides. It is to be noted that hardness data do not provide exact parameter to evaluate wear resistance of cryogenically treated AISI M2 HSS specimen as hardness is apparently less affected by the precipitation of the carbides in the material tested.

The hardness values do not change significantly along the diagonal length of every AISI M2 HSS specimen tested as evident from Fig. 6. From this observation, it can be inferred that cryogenic treatment causes morphological changes in the entire cross section of the material. Evidently, cryogenic treatment is better to all type of coatings as the coatings become futile once it gets removed from the substrate.

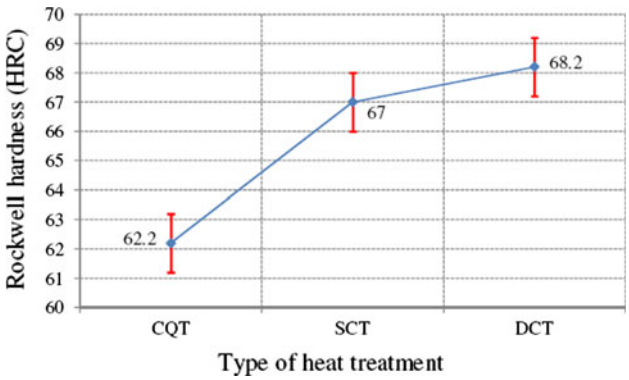

Fig. 6 Hardness values for different types of thermal treatments

3.3 Sliding Wear

Tribological characteristic of AISI M2 HSS specimens were evaluated by performing pin-on-disc sliding wear tests at three different loads using constant speed. The results obtained from the wear tests performed are presented in Table 2. Figure 7 shows the plot of wear rate (W_r) versus normal load for the three types of specimens. It is evident from Fig. 7 that wear rate (W_r) of cryogenically treated (SCT and DCT) specimens is significantly lower than that of the CQT specimens at all the tested normal loads. Compared with the CQT specimens, decrease in wear rate was about 24, 40, and 34% for SCT specimens and about 38, 56, and 58% for DCT specimens at normal load of 49, 68.6, and 88.2 N, respectively. It is interesting to note that decrease in wear rate for SCT and DCT specimens is in general more prominent at higher normal loads as compared to lower normal loads which is also evident from the graph shown in Fig. 7. The DCT specimens outperformed SCT specimens in terms of wear rate by about 19, 26, and 36% at normal load of 49, 68.6, and 88.2 N, respectively. Other very important observation is that the extent of improvement in hardness of DCT specimens over SCT specimens was merely about 1.47%, where as improvement in wear rate varied from 19 to 36% which is

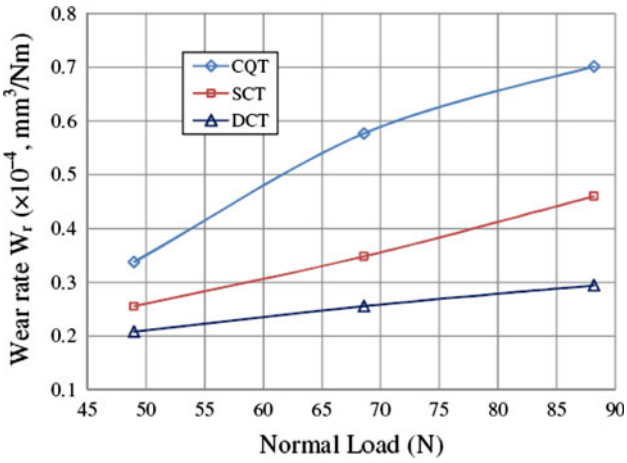

Fig. 7 Variation of estimated wear rate with applied normal load for CQT, SCT, and DCT specimens

Table 2 Tribological characteristics of AISI M2 HSS for pin-on-disc wear tests at 1.5 m/s velocity

Type of heat treatment	Normal load, N	Mean weight loss, g	Wear rate $\times 10^{-4}$ W_r, mm^3/Nm	Wear resistance improvement w.r.t. CQT, %	Wear resistance improvement w.r.t. SCT, %
CQT	49.0	0.081	0.338	…	…
	68.6	0.194	0.577		
	88.2	0.303	0.702		
SCT	49.0	0.059	0.256	24.26	…
	68.6	0.117	0.348	39.68	
	88.2	0.199	0.460	34.47	
DCT	49.0	0.050	0.208	38.46	18.75
	68.6	0.086	0.256	55.63	26.43
	88.2	0.127	0.294	58.11	36.08

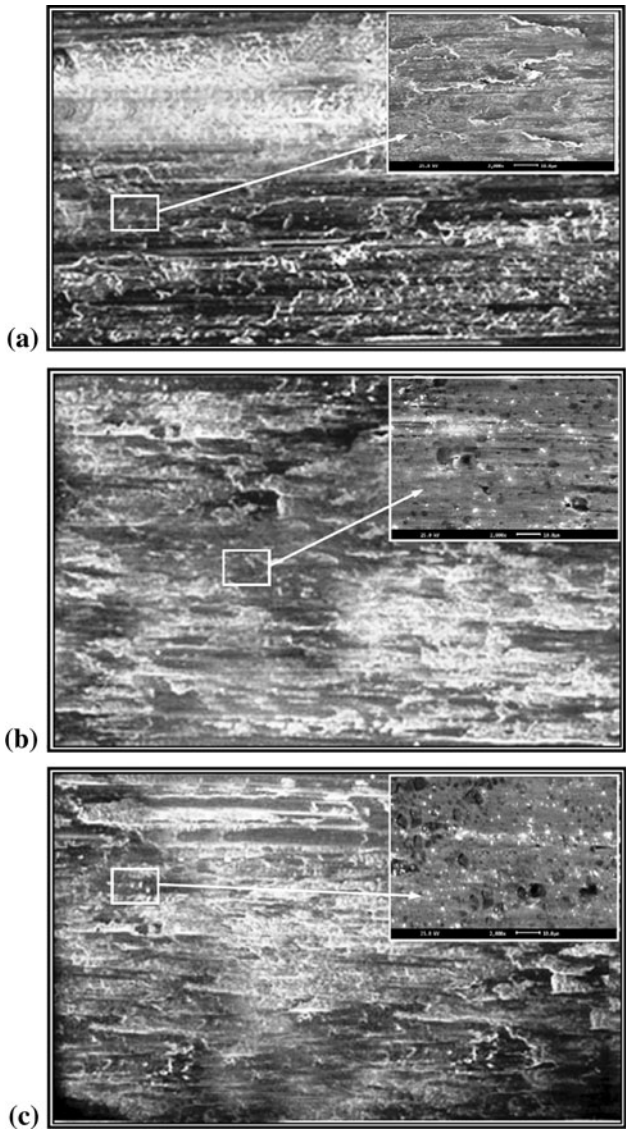

Fig. 8 Optical micrograph of worn surface of (a) CQT, (b) SCT, and (c) DCT specimen. Insets represent the respective SEM micrographs

quite significant. Apparently there is no straight correlation of wear rate with hardness. Hence, it can be concluded that mere hardness data do not provide exact parameter in evaluation of wear resistance of cryogenically treated material. However, it can be accomplished that cryogenic treatment increases the wear resistance of AISI M2 HSS appreciably, but the degree of increase is dependent on the applied load during these tests.

Augmentation of wear resistance by cryogenic treatment (SCT and DCT) is ascribed to the transformation of γ_{RA}, refinement and homogeneous distribution of carbide particles. Figure 8 shows the optical and SEM micrographs (insets) of the worn surfaces of CQT, SCT, and DCT specimens. Under identical wear conditions, worn surfaces of SCT (Fig. 8b) and DCT (Fig. 8c) specimen appear much smoother than the CQT specimen (Fig. 8a). This observation is consistent with the obtained results of wear rates as plotted in Fig. 7. The highest wear rate of CQT specimens is governed by dislodgement of delaminated bands which stretched parallel to the sliding direction resulting in rough surface as is evident from inset of Fig. 8(a). Such high wear rate can be attributed to coarse primary carbides and plastic deformations due to the presence of soft γ_{RA}. Thus, rigorous plastic deformation is considered to be the active wear mechanisms in the CQT specimens. The worn surfaces of the cryogenically treated (SCT and DCT) specimens (insets of Fig. 8b, c) dominated by grooves from where hard carbides had been pulled out and presence of oxides. The grooves and oxides can be identified as black and white dots, respectively, in insets of Fig. 8(b, c). Hence, delamination of carbides coupled with oxidation is the dominating wear mechanism for cryogenically treated (SCT and DCT) specimens.

4. Conclusions

From this study based on mechanical and metallurgical characterization of cryogenically treated AISI M2 HSS, the following conclusions can be drawn:

1. The cryogenic treatment cannot completely transfer the γ_{RA} into martensite. Cryogenic treatment accelerates the precipitation of small secondary carbides, increases their volume fraction and promotes uniform distribution of the carbides in entire bulk of material as compared to CQT AISI M2 HSS.
2. The hardness of AISI M2 HSS increases by 7.76% after subjecting the material to cryogenic treatment. There exists an optimum cryogenic treatment temperature for AISI M2 HSS which may ensure the maximum possible enhancement in hardness. The primary reason that can be attributed for enhanced hardness of AISI M2 HSS is conversion of soft γ_{RA} into relatively hard martensite. Refinement and evenly distribution of secondary carbides also contribute in increasing hardness but at significantly less extent.
3. Both types of cryogenic treatments substantially decrease the wear rate of the AISI M2 HSS compared to the conventional treated ones. However, the improvement in wear rate by deep cryogenic treatment is significantly higher than that achieved by shallow cryogenic treatment.
4. The degree of improvement in wear rate depends on the wear test conditions, which govern the wear mode and mechanism. Rigorous mode of wear is identified as extensive plastic deformation for CQT AISI M2 HSS, whereas mild mode of wear is identified as combined effects of formation of oxides and pull-out of carbides for shallow and DCT AISI M2 HSS.
5. It is inferred that the time and temperature of cryogenic treatment of AISI M2 HSS are critical parameters for obtaining the best combination of desired microstructure and mechanical properties of CQT AISI M2 HSS. Cryogenic treatment can be a better option as compared to surface coatings especially in case of cutting tools as the cryogenically treated AISI M2 HSS tools always retain their improved mechanical properties even after sharpening of cutting edges.

Acknowledgments

This study was supported by the All India Council for Technical Education (AICTE) New Delhi, India by providing grant (F. No: 8023/BOR/RID/RPS-145/2008-2009) under Research Promotion Scheme (RPS). The authors are grateful to the Dr. Durgesh Nadig, Senior Scientific Officer at Centre for Cryogenic Technology, Indian Institute of Sciences, Bangalore, India for assisting the characterization work. The help rendered by Institute of Auto Parts and Hand Tools (IAPT), Ludhiana, India is greatly acknowledged for providing microscopic and cryogenic treatment facilities.

References

1. R.F. Barron, Low Temperature Properties of Engineering Materials, *Cryogenic Systems*, McGraw-Hill, New York, 1996, p 15–23
2. M. Albert, Cutting Tools in the Deep Freeze, *Mod. Mach. Shop.*, 1992, **64**(8), p 55–61
3. T.P. Sweeny, Deep Cryogenics: The Great Cold Debate, *Heat Treat.*, 1986, **18**(2), p 28–32
4. M. Kosmowski, The Promise of Cryogenics, *Carbide Tool J.*, 1981, **4**, p 26–30
5. D.N. Collins, Deep Cryogenic Treatment of Tool Steels, A Review, *Heat Treat. Met.*, 1996, **2**, p 40–42
6. S.S. Gill, H. Singh, R. Singh, and J. Singh, Cryoprocessing of Cutting Tool Materials—A Review, *Int. J. Adv. Manuf. Technol.*, 2010, **48**(1–4), p 175–192
7. S.S. Gill, R. Singh, H. Singh, and J. Singh, Wear Behaviour of Cryogenically Treated Tungsten Carbide Inserts Under Dry and Wet Turning Conditions, *Int. J. Mach. Tools Manuf.*, 2008, **49**(3-4), p 256–260
8. S.S. Gill and J. Singh, Effect of Deep Cryogenic Treatment on Machinability of Titanium Alloy (Ti-6246) in Electric Discharge Drilling, *Mater. Manuf. Process.*, 2010, **25**(6), p 378–385
9. E.S. Zhmud, Improved Tool Life After Shock Cooling, *Met. Sci. Heat Treat.*, 1980, **22**(10), p 3–5
10. A.P. Gulyaev, Improved Methods of Heat Treating High Speed Steels to Improve the Cutting Properties, *Metallurgy*, 1937, **12**, p 65
11. R.F. Barron, Do Treatment at Temperature Below −120°F Help Increase the Wear Resistance of Tool Steels? Here Are Some Research Findings That Indicate They Do, *Heat Treat.*, p 14–17
12. R.F. Barron, Cryogenic Treatments on Metals to Improve Wear Resistance, *Cryogenics*, 1982, **22**, p 409–414
13. R.F. Barron, *Conference of Manufacturing Strategies* (Nashville), Vol. 6, 1986, p 137
14. R.K. Barron, Yes—Cryogenic Treatments Can Save You Money! Here's Why, *Tapi*, 1974, **57**(5), p 35–40
15. F. Meng, K. Tagashira, and H. Sohma, Wear Resistance and Microstructure of Cryogenic Treated Fe-1.4Cr-1C Bearing Steel, *Scr. Metall. Mater.*, 1994, **31**, p 865–868
16. F. Meng, K. Tagashira, R. Azuma, and H. Sohma, Role of Eta-Carbide Precipitations in the Wear Resistance Improvements of Fe-12Cr-Mo-V-1.4C Tool Steel by Cryogenic Treatment, *ISIJ Int.*, 1994, **34**, p 205–210
17. D. Mohan Lal, S. Renganarayanan, and A. Kalanidhi, Cryogenic Treatment to Argument Wear Resistance of Tool and Die Steels, *Cryogenics*, 2001, **41**, p 149–155
18. A. Molinari, M. Pellizzari, S. Gialanella, G. Straffelini, and K.H. Stiasny, Effect of Deep Cryogenic Treatment on the Mechanical Properties of Tool Steels, *J. Mater. Process. Technol.*, 2001, **118**, p 350–355
19. J.Y. Huang, Y.T. Zhu, X.Z. Liao, I.J. Beyerlein, M.A. Bourke, and T.E. Mitchell, Microstructure of Cryogenic Treated M2 Tool Steel, *Mater. Sci. Eng. A*, 2003, **339**, p 241–244
20. V. Leskovsek, M. Kalin, and J. Vizintin, Influence of Deep Cryogenic Treatment on Wear Resistance of Vacuum Heat-Treated HSS, *Vacuum*, 2006, **80**, p 507–518
21. F.J. de Silva, S.D. Franco, A.R. Machado, E.O. Ezugwu, and A.M. Souza, Jr., Performance of Cryogenically Treated HSS Tools, *Wear*, 2006, **261**, p 674–685
22. D. Yun, L. Xiaoping, and X. Hongshen, Deep Cryogenic Treatment of High-Speed Steel and Its Mechanism, *Heat Treat. Met.*, 1998, **3**, p 55–59
23. ASTMG99-05, "Standard Test Method for Wear Testing with a Pin-on-Disk Apparatus," *ASTM Book of Standards*, V 03.02, West Conshohocken, PA, 2005
24. D. Das, A.K. Dutta, V. Toppo, and K.K. Ray, The Effect of Cryogenic Treatment on the Carbide Precipitation and Tribological Behavior of D2 Steel, *Mater. Manuf. Process.*, 2007, **22**, p 474–480
25. P.M. Unterweiser, H.E. Boyer, and J.J. Kubbs, Ed., *Hear Treater's Guide*, ASM, Metal Park, OH, 1987, p 300